Thermal Science and Engineering 2024, 7(3), 8671.
https://doi.org/10.24294/tse.v7i3.8671

Article

Relating alkali release from a wood pellet with combustion progress: A modified random pore model supportive study

Rudolf P. W. J. Struis[1,2,*], Marco Wellinger[1,3], Christian Ludwig[1,2]

[1] PSI Center for Energy and Environmental Sciences, LEP CPM, Paul Scherrer Institute (PSI), 5232 Villigen PSI, Switzerland
[2] School of Architecture, Civil and Environmental Engineering, ENAC IIE GR-LUD Station 2, École Polytechnique Fédérale de Lausanne (EPFL), 1015 Lausanne, Switzerland
[3] Institute of Chemistry and Biological Chemistry, Coffee Excellence Center, Zurich University of Applied Sciences (ZHAW), 8820 Wädenswil, Switzerland
*** Corresponding author:** Rudolf P. W. J. Struis, rudolf.struis@psi.ch, rudolfstruis@ursulaburgherr.ch

CITATION

Struis RPWJ, Wellinger M, Ludwig C. Relating alkali release from a wood pellet with combustion progress: A modified random pore model supportive study. Thermal Science and Engineering. 2024; 7(3): 8671.
https://doi.org/10.24294/tse.v7i3.8671

ARTICLE INFO

Received: 10 July 2024
Accepted: 16 August 2024
Available online: 23 August 2024

Abstract: This paper concerns a miniature gasifier fed with a constant ambient-pressure flow of air to study the pyrolysis and subsequent combustion stage of a single wood pellet at T = 800 °C. The alkali release and the concentration of simple gases were recorded simultaneously using an improved alkali surface ionisation detector and a mass spectrometer in time steps of 1 s and 1.2 s, respectively. It showed alkali release during both stages. During combustion, the MS data showed almost complete oxidation of the charred pellet to CO_2. The derived alkali release, "O_2 consumed", and "CO_2 produced" conversion rates all indicated very similar temporal growth and coalescence features with respect to the varying char pore surface area underlying the original random pore model of Bhatia and Perlmutter. But, also large, rapid signal accelerations near the end and marked peak-tails with O_2 and CO_2 after that, but not with the alkali release data. The latter features appear indicative of alkali–deprived char attributable to the preceding pyrolysis with flowing air. Except for the peak-tails, all other features were reproduced well with the modified model equations of Struis et al. and the parameter values resembled closely those reported for fir charcoal gasified with CO_2 at T = 800 °C.

Keywords: wood pellet; pyrolysis; combustion; alkalis; surface ionisation detector; random pore model; alkali deprivation

1. Introduction

When using natural or waste wood in thermo-chemical conversion processes, a number of heteroatoms (e.g., sulfur, chlorine, mainly potassium, with or without metal contaminants) may hinder the processes, as well as, pose a threat to equipment and/or the environment. Due to the often strongly heterogeneous composition of the feedstocks and high dynamics of thermo-chemical reactions, the elemental concentrations in process gases show a high temporal variability. In order to accurately characterize such changes, efficient and representative sampling methods and analytical instruments with a high sensitivity and time resolution are necessary. To this purpose, a miniature thermo-chemical reactor (MTR) had been developed and constructed at PSI to study the pyrolysis and subsequent combustion of single commercial-sized wood pellets under a constant flow of ambient-pressure air at T = 800 °C. During the run, the amount of alkalis released with the reactor gas was monitored using an improved alkali surface ionisation detector (SID II) in time steps of about 1 s, and the evolution of simple gases by mass-to-charge ratios recorded

with a MS every 1.2 s. After several numerically executed steps and conversions (see further on), the resulting alkali release, "O_2 consumed" and "CO_2 produced" rate course data with the combustion-specific stage were each compared in view of the modified random pore model of Struis et al. [1] and with the weight loss data of wood char from a pre-pyrolysed fir lath piece recorded during gasification with CO_2 at T = 800 °C in a TGA [1–3].

Thermo-chemical conversion processes with woody feedstock

During thermal conversion of woody feedstock, four stages can occur consecutively as a function of time with increasing temperature [4,5]:

(1) Heating and drying (up to T = 200 °C). (2) Pyrolysis (starting from T = 200 °C) by thermal decomposition of biomass macromolecules in the absence of an oxidant. (3) Gasifcation (starting from T = 400 °C) by partial oxidation by an understochiometric amount of oxidant. Or, (4) Combustion (starting here from T = 800 °C) by exhaustive oxidation with at least a stoichiometric amount of oxidant. Clearly, also overlap between stages (2–4) does occur. The four stages are depicted in **Figure 1**, including simple volatile components evolving from drying, pyrolysis, gasification, or combustion, towards the formation of wood ash at the end. The figure also shows another fresh wood pellet before combustion in air (λ = air-to-fuel ratio), after drying, after pyrolysis in N_2, and the wood ash at the end.

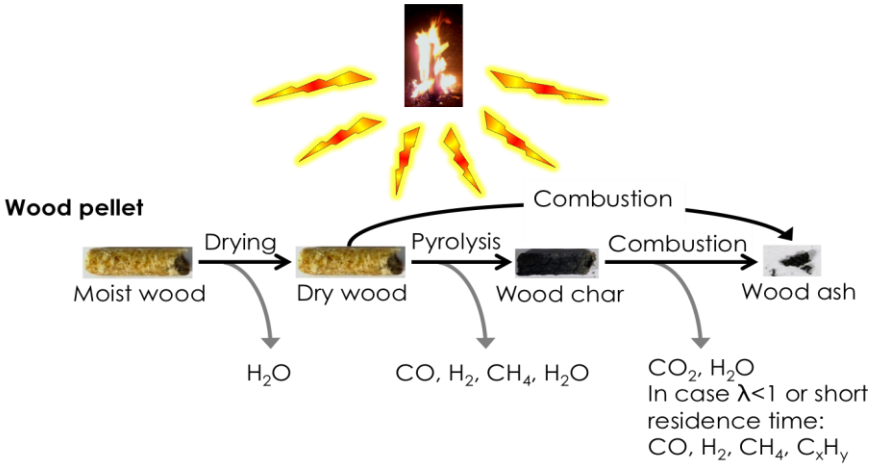

Figure 1. Stages of thermo-chemical conversion of a wood pellet.

2. Materials and methods

2.1. Chemical physical characteristics of the wood pellets

The wood pellets were bought from Buerli Trocknungsanlage (drying plant), Alberswil, Switzerland [6]. The pellets have a density of 1.2 kg/dm^3, a diameter of 6 mm, a length of around 2 cm, and water content below 10% by weight. A pellet weighing 0.70 ± 0.01 g was selected for the miniature gasifier run and with more pellets in other runs using a bubbling fluidized bed gasifier. The chemical composition of the wood pellet batch in question with respect to C, H, O, N, S, Cl, K, and Na is shown in **Table 1**. The pellet composition agrees well with that of most

temperate-climate woods. It also shows that potassium is the predominant alkali element.

Table 1. Chemical composition of the wood pellets used in this work (C, H, O, N, S from Wellinger et al. [7], together with own results for K and Na with wood pellet ash.

Element concentration of the wood pellets	
C [Wt.-%]	47.31
H [Wt.-%]	6.23
O [Wt.-%]	44.44
N [Wt.-%]	0.18
S [Wt.-%]	0.01
Cl [Wt.-%]	< 0.02
K [µg/g]	551
Na [µg/g]	28

2.2. Overview of the experimental, sampling and measuring setup

The miniature thermo-chemical reactor (MTR, or simply "miniature gasifier"), alkali ionisation detector (SID II), continuous gas washer, and MS were setup according to the flow sheet shown in **Figure 2**. The gasification run was performed with a 750 ml_N/min flow of air under atmospheric pressure at room temperature. The air was supplied by an in-house filtering and compressor unit fed with ambient air. The air flow was led to the heated MTR. After stabilisation of gas flow and gasification temperature (T = 800 °C) with the MTR, one wood pellet was injected into the reactor through a vertical drop. Because a short length of sampling line is crucial when conducting direct gas measurements, the SID II was placed within 0.5 m distance from the gas outlet of the reactor. The remaining part of the reactor gas was directed to the continuous gas washer, operated at low temperature (T = −10 °C) and elevated pressure (P < 5 bar), to separate particulate and condensable matter. The non-volatile ("permanent") gases remaining after washing were then transported through sampling lines to the SID II and the MS, and they did neither affect the alkali nor the non-volatile gas transport efficiency.

2.3. Miniature thermo-chemical reactor

The design, construction, and experiments with a novel single pellet gasifier were the scope of the PhD thesis of Johannes and Judex at PSI [8]. The reactor was made from Inconel® to withstand the high temperatures during the run. The reaction chamber has a diameter of 16 mm and a height of 100 mm. The MTR is positioned inside a cylindrical furnace that can be heated electrically to the desired temperature to maximally T = 970 °C. The gasification agent (here ambient air) enters from the bottom through a distributor that at the same time serves as grate for the pellet. The reactor is placed in a vertical cylindrical cavity of a ceramic oven (Micromeritics, 48 V, 350 W). Reactor gas outlet and thermocouple inlet are positioned above the ceramic oven. The reactor temperature is measured by a thermocouple (Type K) with its tip positioned about 2 cm above the fuel grate within the reactor cavity. The wood

pellet is given into a lock hopper above the reactor. When the temperature and all sensors are stable, the pellet is released through a ball valve and reaches the reactor grid in less than 30 s to avoid heating the pellet prematurely.

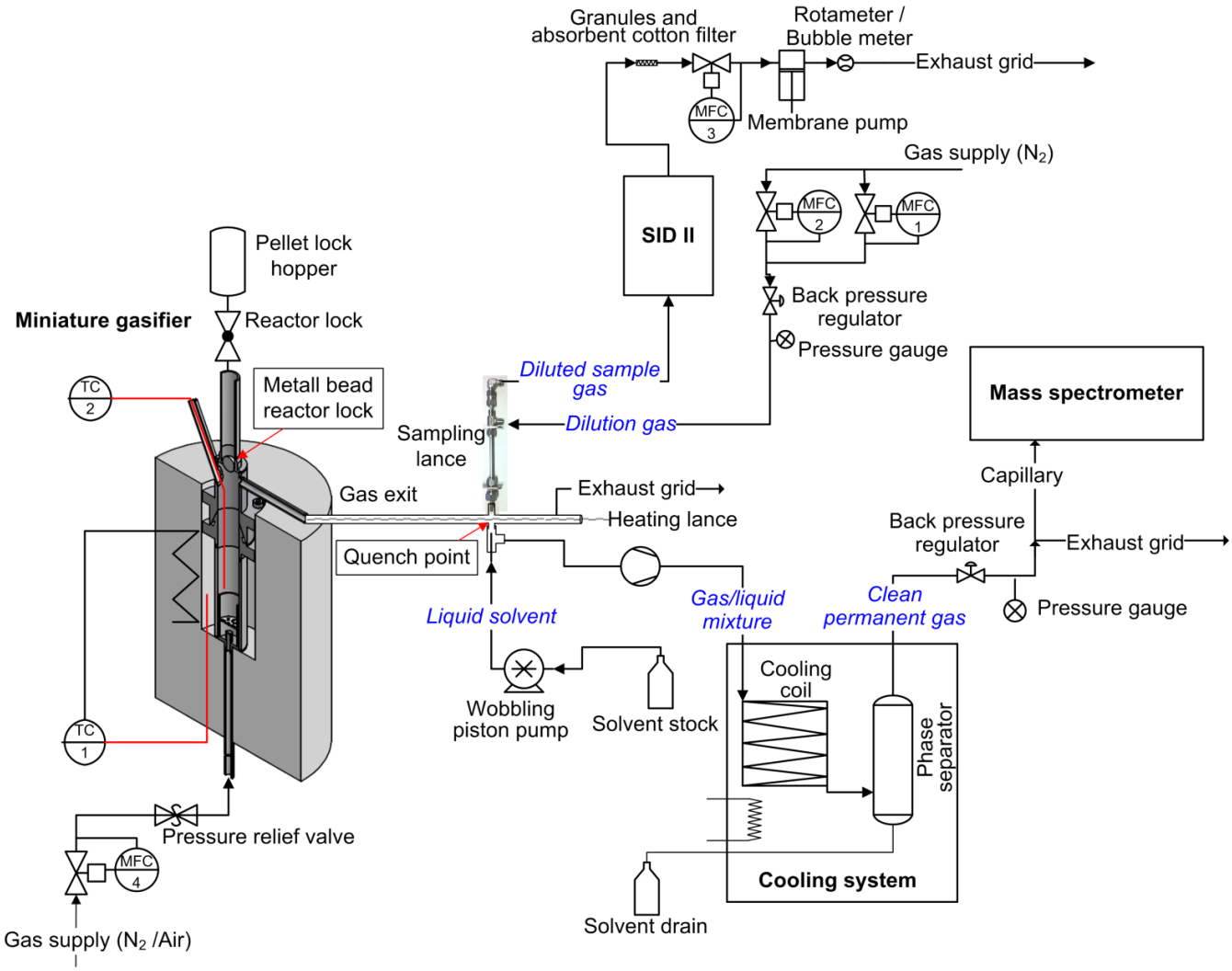

Figure 2. Flow sheet of the miniature gasifier including the sampling and measurement setup.

After that, a ferromagnetic ball is released to reduce any additional dead volume for the outgoing reactor gases. Lastly, the ball valve is closed again to provide additional sealing along with the cover nut. The pellet thus experiences similar conditions as if it had entered a large gasifier. The product gas leaves the reactor at the top through a sampling line heated to approximately T = 300 °C to prevent the condensation of tars. After each experiment, the grate was removed, the ash recovered, and the reactor cleaned. More details can be found in the literature [8,9].

2.4. Improved surface ionization detection (SID II)

The SID II is a newly developed alkali detector based on the principle of surface ionisation occurring by their impingement on a hot platinum filament, followed by acceleration of the ions by the voltage difference between filament and collector, and the detection of the ion current at the collector grating. Further details can be found in Judex [8] and Wellinger's works [9]. The detector signals are

typically in the order of nano-amperes (nA). The alkali detector had demonstrated high sensitivity over 4 orders of magnitude [8,9]. The signal value depends on the effective volume flow carrying the alkalis and somewhat also on the bulk gas composition. Power law correlations were established to represent the measured signals accurately. Two correlations applicable for sodium and potassium nitrates nebulised at concentrations of 0.7, 7, and 70 $\mu g/m_N^3$ in air and in nitrogen, respectively, had already been published [9]. In order to exploit the alkali concentration validity range of the power law correlations, the gas from the reactor was diluted with a constant volume flow of N_2 prior to entering the SID II. The sample gas dilution setup and the sampling lance developed for SID II have been described elsewhere [7,9].

The principle of the sensor is based on the high probability of some alkali metals getting ionised during the desorption process from the ionising filament [10]. The sensor is especially sensitive to potassium (K), sodium (Na), and caesium (Cs) [11]. With our wood pellet, the concentration of K surmounts that of Na by a factor of 20 (**Table 1**), and the amount of Cs is normally negligibly small (<1 ppm [12]).

2.5. Continuous gas washer

After the SID II, a continuous gas washer (**Figure 2**) similar to the one described by Kowalski et al. [13] was used to separate water, soot, and tars from the permanent gases before being led to the MS. With the continuous gas washer, the raw gas was mixed thoroughly with water-containing organic solvent and transported to a two-phase separator unit operating at a below-zero temperature (T = −10 °C) under the pressure (P < 5 bar). The cleaned gas consists of "permanent" species that did not condensate out, and it led to the MS. In this study, 1-methoxy-2-propanol ($C_4H_{10}O_2$, CAS-Nr.107-98-2) was used as solvent, because of its much higher capability to solubilise tars in comparison to pure water. This is particularly important when analysing producer gas from pilot or industrial biomass gasifiers with high tar loads.

2.6. Mass spectrometer

The MS was a "Pfeiffer Thermostar" with a sample flow of approx. 1–2 ml_N/min depending on the pressure conditions at the capillary inlet. The built-in secondary electron multiplier was used as the detection system. For the present study, the mass signals for H_2^+(m/z = 2), N_2^+ and CO^+(m/z = 28), O_2^+(m/z = 32), Ar^+(m/z = 40), and CO_2^+(m/z = 44) were selected to reconstruct the true reactor gas composition and amounts as a function of the experimental runtime. Under constant ambient pressure at the capillary inlet, the MS takes in a constant amount of sample gas from the reactor. When consumption or production occurs during the thermo-chemical conversion experiment, the gas flow alters. To convert the relative intensities measured by the MS into intensities that are proportional to the absolute flow from the reactor, argon (m/z = 40) in the air fed to the MTR with air was used as an internal, non-reactive, gaseous standard agent ("tracer") to compensate for total flow changes, as follows: The Ar signal intensity before the start of the experiment was used as a reference signal intensity. The recorded Ar signal intensity for each

point in time was then divided by the reference signal intensity. This yielded ratio values ranging between 1.02 (ideally 1.00) before inserting the pellet into the reactor to 0.88 minimally during pyrolysis of the wood pellet. The Ar ratio values were then used to correct the other measured MS [m/z] intensities by dividing the MS-data by the Ar ratio data on a comparable runtime basis. As last step, the dilution-corrected MS data were converted into relative volume amounts (%V/V) after having experimentally established the proportionality ratio between simultaneously recorded MS (in arbitrary units) and pre-calibrated Varian micro-GC (%V) values with each gas species of interest during gasification runs with wood pellets with air in a bubbling fluidized bed reactor at T = 755 °C [9].

2.7. Modified Random Pore Model (MRPM)

Struis et al. [1] derived kinetic relations by modification of the original random pore model (RPM) of Bhatia and Perlmutter [14]. The original RPM addressed the conversion degree, *X*, the conversion-time behaviour, *X(t)*, and the conversion progress rate, d*X*/dt, of a solid-gas reaction with a carbonaceous porous solid in terms of the variation in the reaction surface area, *S*. The original model uses two parameters (A_0, ψ) to describe or reproduce the behaviour of a system that either shows one or no maximum in the derived conversion progress rate with runtime. A_o denotes the experimentally accessible reaction rate at start, and ψ comprises details regarding the pore system. The maximum in d*X*/d*t* (=*S*/S_0) with conversion degree is attributed to two opposing effects: pore growth increases the reaction surface area, and pore coalescence at intersections decreases the reaction surface area. In the work of Struis et al. [1, 2], and that of other workers [15,16], the conversion progress, *X*, is connected with the weight of the porous char sample, *M*, according to:

$$X(t) = (M_0 - M(t))/(M_0 - M_{ash}) \quad (1)$$

here, M_0 denotes the char weight at the start of the gasification, M_{ash} stands for the weight of the bottom ash after complete conversion, and *M(t)* is the weight at a run time t. Accordingly, *X(t)* is zero at start and attains unity at completion of the mass conversion. The conversion progress rate, dX/d*t*, can principally also be interrelated with other quantities associated with the char-gas reaction, such as the amount of oxidant gas consumed (here, O_2), the amount of product gas produced (here, mainly CO_2), and the release of biomass-native alkali from the sample (here, one wood pellet). Under kinetic control and ignoring the reaction on the exterior woody particle surface, the kinetic equations modified by Struis et al. [1] are defined by correlation time, τ', and conversion rate progress, *X*, as given in Equation (2) and Equation (3), respectively:

$$\tau' = A_0 t[1 + (Bt)^P] \quad (2)$$

$$X = 1 - e^{-\tau'\left(1+\frac{\psi\tau'}{4}\right)} \quad (3)$$

In Equation (2), τ' is a dimensionless run time, t the experimental run time, A_0 the experimentally accessible initial reaction rate, Ψ the pore system related structural constant, *B* a reciprocal time constant, and *P* a dimensionless power law constant. After differentiating Equation (3) with respect to time *t*, the resulting rate reads [1]:

$$\frac{\mathrm{d}X}{\mathrm{dt}} = \mathrm{A}_0(1 + (P+1)(Bt)^P)(1-X)\sqrt{1 - \psi\ln(1-X)} \quad (4)$$

Noteworthy, the three modified equations converge to the original ones from Bhatia and Perlmutter when fixing $B = 0$.

2.8. Data treatment of selected MS gas data for model analysis

Figure 3 shows a compilation of the raw alkali signal from SID II in nano-Ampere, [nA], the temperature [°C] inside the reactor, and the MS signals for selected gases, as a function of the experimental runtime, with the single wood pellet at T = 800 °C. **Figure 3** shows H_2 (m/z = 2), O_2 (m/z = 32), CO and N_2 (both m/z = 28), and CO_2 (m/z = 44) in the MS machine units after having been corrected for gas dilution effects.

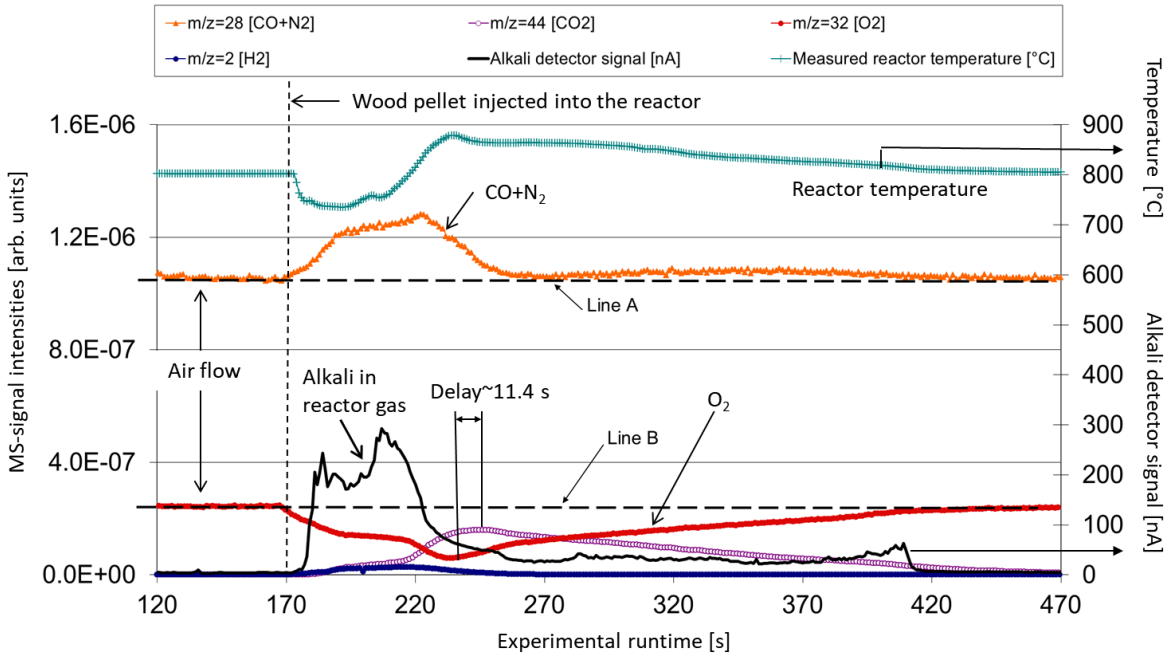

Figure 3. Raw data compilation of the amount of alkalis detected with the reactor gas, the reactor temperature, MS signals for m/z = 28 (CO + N_2), m/z = 32 (O_2), and other gases, recorded during the thermo-chemical conversion run of a single wood pellet at T = 800 °C in a constant flow of air.

After pellet injection, the CO_2 and O_2 courses with runtime progress in a complementary manner in that the O_2 signal passes through a minimum at $t \approx 233$ s, whereas CO_2 shows a maximum, but later at $t \approx 244$ s. The delay is likely caused by the moderate affinity of CO_2 with the liquid quench solvent (1-methoxy-2-propanol), as also noticed in other studies with the continuous gas washer [17,18]. The anomaly in runtime was not detected with the other gases. Hence, the "dwell time" of CO_2 was corrected by subtracting 10.5 s from the experimental runtimes.

The amounts of "CO produced" and "O_2 consumed" were obtained by subtracting the constant N_2 and O_2 levels pertaining to clean air for and after the experimental run (**Figure 2**) and then multiplying the resulting O_2 values with −1. The released alkali amounts and the amounts of "O_2 consumed", H_2, CO, CH_4, and "CO_2 produced" were each converted to calibrated units (Section 2.6). The values of "dX (O_2 consumed)/dt" and "dX (CO_2 produced)/dt" with the combustion stage were

first averaged as follows: To suppress the impact from experimental noise with the calibrated MS data, two data blocks with one data point in between were used. Each data block comprised nine successive {*t*, *X(t)*} data points. Instead of using two adjacent data points, block-averaged values were used to calculate *dX/dt*, and the result was allocated with the time value of the data point between the blocks. The procedure was repeated by moving the blocks plus intermediate data point one position forward in time, and so on, till reaching the end of the experimental data set in question.

Lastly, with gasification runs with more pellets in a fluidized bubble-bed gasifier under ideal gas solvent quench conditions, it was reported that the gas-phase "downstream/upstream" ratio with CO_2 could only be kept between 0.9–1, whereas those of H_2, CO, and CH_4 were much better (ratios~1) [17,18]. This was also evidenced in this study by comparing the calibrated "O_2 consumed" and "CO_2 produced" data where they reflected complete combustion, i.e., $C_{char} + O_2 \rightarrow CO_2$ and CO absent. Although the differences were small, the data overlay (not shown here) was not consistent enough ([O_2 consumed] ≠ [CO_2 produced]), but the differences diminished at higher runtimes. The anomaly was overcome by multiplying the "CO_2 consumed" values with 1.035.

2.9. Experimental point of reference with the MRPM analysis

The point of reference for comparing the temporal alkali and gas rate courses and model parameters obtained in this study were the model parameters for the mass loss conversion rate (Equation (1)) with pre-pyrolysed and grinded charcoal particles prepared from one fir lath (without bark). About 10 mg charcoal was gasified with CO_2 at T = 800 °C in a TGA. In contrast with the wood pellet, the fir charcoal was obtained in two consecutive stages: Pre-pyrolysis (2.5 h at T = 600 °C under Ar flow) and post-pyrolysis (20 min at T = 900 °C under He flow) [1,2]. Notwithstanding these, a comparison is fair in that the certified wood pellet batch comprises a high amount of heartwood among less sapwood, bark, branches or twigs. In the literature, the modified RPM equations were found applicable with several tree woods, chars, and charcoals. The reference sample is hereafter named "fir charcoal".

3. Results and discussion

3.1. Chemical and physical transients during the wood pellet gasification

For better visibility, the two apparent stages with the gasification run are shown separately in **Figure 4A**,**B**, respectively. It must also be mentioned that the alkali release is now shown in the calibrated unit of [mg/m_N^3], and "O_2 consumed", H_2, CH_4, CO_2, and "O_2 consumed" in the calibrated [%V/V] unit.

With the pyrolysis stage (**Figure 4A**), the tentatively drawn broken line with the temperature progresses rather smoothly with runtime. In chronological order, it depicts the arrival of the wood pellet in the reactor cavity by a fast temperature drop; the temperature passes through a minimum, and recovers again by the heat produced from the combustion of outflowing flammable gases and possibly also less

combustion resistant wood pellet constituents. After that, the temperature even surpasses the pre-settled reactor temperature (T = 800 °C), passes through a maximum, and then converges slowly to a temperature of T ≈ 860 °C around runtime ~280 s. The tentative temperature course also emphasizes transient's features, such as water evaporation with the pellet (A), wood depolymerisation (D), and presumably also combustion of lignin (C) mobilized with the manufacturing of the wood pellets to "glue" the wood particles during the pelletization process together.

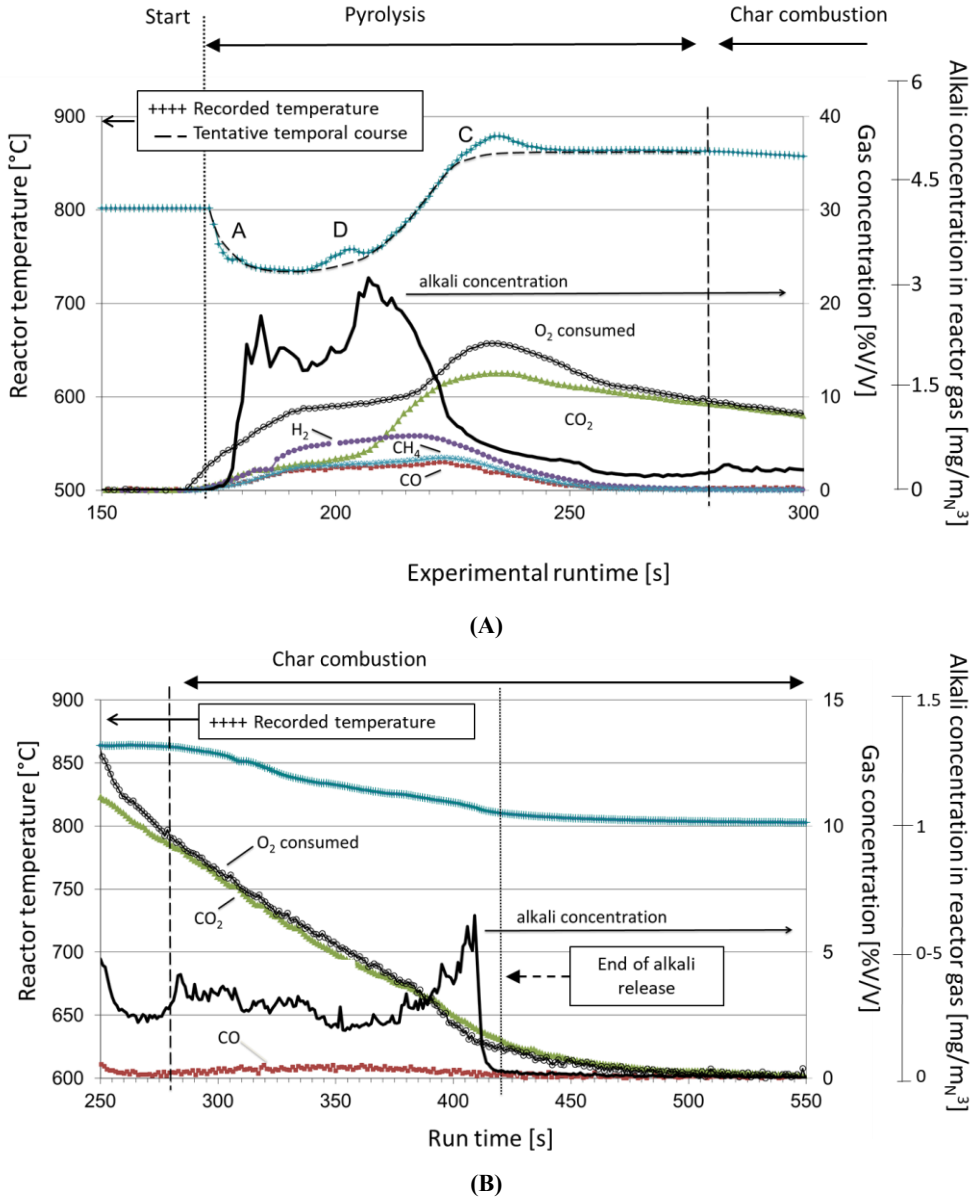

Figure 4. (A) Measured and tentative reactor temperature course as a function of the experimental run time. Also shown are the amount of alkalis detected in the reactor gas [mg/m_N^3], the amount of "O_2 consumed", and several other evolving gases (H_2, CO, CO_2, CH_4) in [%V/V]; **(B)** Continuation of the data shown with **Figure 4A** with extended, enlarged axis scales.

Particulates from sawmills and planning works [7]. The temperature stabilization around runtime ~280 s coincided with the absence of CO, H_2, and CH_4

with the reactor gas, whereas the signals of "CO_2 produced" and "O_2 consumed" continued.

In **Figure 4B**, the reactor temperature in the alleged sole char combustion stage converged gradually from T ≈ 860 °C (runtime ~280 s) to a stable temperature laying slightly above T = 800 °C for runtimes > 500 s. With [CO] much smaller than [CO_2, it reflects near complete combustion of the charred wood pellet with O_2.

Lastly, a large alkali release started jointly with the outflow of flammable gases from the wood pellet during the pyrolysis stage (**Figure 4A**). The alkali release continued during the combustion stage (**Figure 4B**), but in much smaller amounts. (Note that the alkali unit scale range with **Figure 4A** is 4 times larger than with **Figure 4B**).

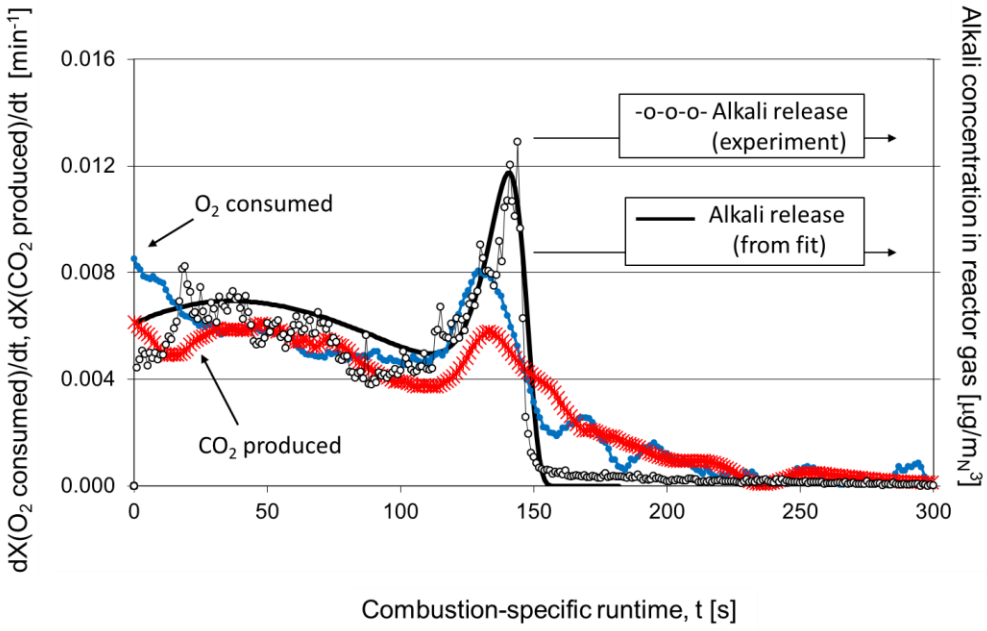

Figure 5. Overlay of measured (-o-) and fitted alkali release data (solid line using Equtions (2–4)) together with "O_2 consumption" and "CO_2 production" rates derived from MS data recorded simultaneously during the combustion stage of the wood pellet under a constant air flow at T = 800 °C.

3.2. Relating the alkali release to product gas reaction rates

Figure 5 shows the alkali concentration with the reactor gas, as a function of the combustion-specific runtime ($t_{combustion}$ = 0). The start time was chosen where, with **Figures 4A,B**, the O_2 and CO_2 concentrations predominated in the near absence of any other pyrolysis or combustion product gases. Here, the start of the pellet combustion stage was arbitrarily fixed at the experimental runtime = 280 s. Modelling the alkali release data, an additional parameter was added to multiply the integral right-hand side of Equation (4) to prevent compromising the original meaning of parameter A_0 as the reaction rate with the initial char(coal) pore surface area [1,14].

With **Figure 5**, the drawn solid black line shows the reproduced temporal course of the alkali release by the MRPM for the parameters shown in **Table 2**. With

Table 2, the unit for A_0 and B with the wood pellet is [s^{-1}], and with the fir charcoal [min^{-1}] because O_2 is more reactive than CO_2. The data reproduction quality with the alkali release data was satisfactory, except for the minute peak-tail at the end that lasted till about $t_{combustion}$ ~300 s.

Table 2. Model parameters derived for Equation (4) with the temporal alkali release of a charred wood pellet during combustion in flowing air at T = 800 ℃, and from the weight loss of pre-pyrolysed fir charcoal during gasification with CO_2 at T = 800 ℃ [1]. Standard (1σ) errors were provided by the modelling software.

Sample	**Parameter's quantity**	**Numerical data multiplication factor**	A_0	ψ	B	P
Charred wood	Alkali release	44607	0.00609	4.5	0.00669	18.6
Pellet (this study)	(Single run)	± 378	±0.00017 [s^{-1}]	±0.4 [-]	± 0.00002 [s^{-1}]	±0.6 [-]
Fir charcoal [1]	Weight loss	Not applicable	0.0056	5.0	0.0051	14.4
	(18 experiments)		±0.0013 [min^{-1}]	±0.2 [-]	± 0.0003 [min^{-1}]	±1.6 [-]

Also shown with **Figure 5** are the "O_2 produced" and the "CO_2 consumed" dx/dt rate data (in their own calibrated units). The gas axis values were chosen such to achieve a high visually possible overlay (coverage) with the alkali release data. All three data sets revealed typically the same features (**Figure 5**), except for deviations with $t_{combustion}$ < 23 s attributable to overlap with the preceding pyrolysis domain, and by a very small peak-tailing signal remaining after the decline of the taller, but shorter-lived, alkali release peak. The peak-tail began after $t_{combustion}$ ~140 s and lasted for at least 100 s after that. Actually, similarly small signal-tais and time durations were also found with the raw MS data with the gases, except for CO and CO_2 in that they showed substantially larger tail amplitudes. Striking also is that both the CO and CO_2 dX/dt signal-tails appeared as soon as the accelerated alkali release had ceased at $t_{combustion}$ ~140 s (**Figure 5**).

The different peak-tail amplitudes with the alkali release and the CO and CO_2 conversion rates during the combustion stage may be understood by the difference in reactivity of the flowing gas during the pyrolysis treatment in this study (reactive O_2) and with fir charcoal (inert Ar and He). The fir lath was destined for construction purposes, so it essentially consists of heartwood. In contrast with oxygen, pyrolysis in flowing, non-reactive gas at sufficiently high temperatures mainly enables the outflow of decomposition gases from woody samples, but hardly any combustion. Therefore, the alkalis with the fir heartwood are hardly depleted with the charcoal, where this could very well be the case with the wood pellet pyrolysis under O_2. This would also explain the fact that the alkali release with the charred wood pellet seems to have run out prematurely (**Figure 5**), and, as a result, the large signal-tail-amplitude with O_2 and CO_2 started where the alkali release had stopped. Noteworthy, the almost doubling of the effective combustion duration with the pellet char here was reported found with the fir charcoal that had been deprived of its alkali by washing them out with HCl [1].

Author contributions: Conceptualization, MW and CL; methodology, MW; software (curve fitting), RPWJS; validation, RPWJS and MW; formal analysis,

RPWJS and MW; investigation, RPWJS and MW; resources, CL; data curation, RPWJS and MW; writing—original draft preparation, MW; writing—review and editing, RPWJS, MW and CL; visualization, MW; supervision, CL; project administration, CL; funding acquisition, CL. All authors have read and agreed to the published version of the manuscript.

Acknowledgments: In the very early stages of this project, financial support was obtained from Swisselectric research (Project TREPGAS) and the Swiss Federal Office of Energy (Project 102093). The authors also thank Johannes W. Judex for instructions regarding the miniature thermo-chemical reactor (MTR) and assisting the quantification of the MS data for main reactor gas components by simultaneous use of a calibrated micro-GC and a MS during bubbling fluidised bed test rig experiments with wood pellets. We are also grateful to Serge Biollaz (PSI) and his research group for valuable discussions and providing equipment, such as the continuous gas washer unit, and more.

Conflict of interest: The authors declare no conflict of interest.

Abbreviations

MS	Mass spectrometer
MTR	Miniature thermochemical reactor ("Miniature gasifyer")
RPM	Random pore model
MRPM	Modified random pore model by Struis et al. [1]
SID II	Improved surface ionisation detector developed at PSI
TGA	Thermogravimetric analyser

Notation

A_0	Experimental initial reaction rate defined in Equation (2), min^{-1}
B	Modified model parameter introduced in Equation (2), min^{-1}
M_{ash}	Mass of ash, g
$M(t)$	Char coal mass at gasification time t, g
P	Power law constant with Equation (2), dimensionless
S	Active surface area per unit volume, m^2/m^3
t	Experimental run time, min
T	Temperature, °C
X	Conversion progress degree or burn-off, dimensionless

Greek letters

τ'	Correlation time defined with Equation (2), dimensionless
Ψ	Pore system parameter defined with Equation (3), dimensionless

Subscript

0	Initial, at start of the pellet gasification run

References

1. Struis RPWJ, von Scala C, Stucki S, Prins R. Gasification reactivity of char coal with CO_2. Part I: Conversion and structural phenomena. Chemical Engineering Science. 2002; 57(17): 3581-3592. doi: 10.1016/S0009-2509(02)00254-3
2. Struis RPWJ, von Scala C, Stucki S, Prins R. Gasification reactivity of char coal with CO_2. Part II: Metal catalysis as a function of conversion. Chemical Engineering Science. 2002; 57(17): 3593-3602. doi: 10.1016/S0009-2509(02)00255-5
3. Struis RPWJ, von Scala C, Stucki S, Prins R. In: Bridgwater AV (editor). Progress in Thermochemical Biomass Conversion. Blackwell Science Ltd.; 2001. Volume 1, pp. 73-91.
4. Higman C, van der Burgt M. Gasification Processes. Gasification. Published online 2008: 91-191. doi: 10.1016/b978-0-7506-8528-3.00005-5
5. Kaltschmitt M, Thrän D, Smith KR. Renewable Energy from Biomass. Encyclopedia of Physical Science and Technology. Published online 2003: 203-228. doi: 10.1016/b0-12-227410-5/00059-4
6. Ecological product from native forests—Pellet production. Available online: http://www.buerli-pellets.ch/herstellung (accessed on 20 August 2024).
7. Wellinger M. Development and Application of Devices for Online Trace Element Analysis of Thermal Process Gases from Woody Feedstocks [PhD thesis]. École polytechnique fédérale de Lausanne EPFL; 2012.
8. Judex, Johannes W. Grass for power generation: extending the fuel flexibility for IGCC power plants. Published online 2010. doi: 10.3929/ETHZ-A-006032252
9. Wellinger M, Biollaz S, Wochele J, et al. Sampling and Online Analysis of Alkalis in Thermal Process Gases with a Novel Surface Ionization Detector. Energy & Fuels. 2011; 25(9): 4163-4171. doi: 10.1021/ef200811q
10. Jäglid U, Olsson JG, Pettersson JBC. Detection of sodium and potassium salt particles using surface ionization at atmospheric pressure. Journal of Aerosol Science. 1996; 27(6): 967977. doi: 10.1016/0021-8502(96)00025-0
11. Svane M, Hagström M, Davidsson KO, et al. Cesium as a Tracer for Alkali Processes in a Circulating Fluidized Bed Reactor. Energy & Fuels. 2006; 20(3): 979-985. doi: 10.1021/ef0502731
12. Thy P, Lesher CE, Jenkins BM, et al. Trace Metal Mobilization During Combustion of Biomass Fuels. UC Berkeley; 2007.
13. Kowalski T, Judex J, Schildhauer TJ, et al. Transmission of Alkali Aerosols through Sampling Systems. Chemical Engineering & Technology. 2010; 34(1): 42-48. doi: 10.1002/ceat.201000366
14. Bhatia SK, Perlmutter DD. A random pore model for fluid-solid reactions: I. Isothermal, kinetic control. AIChE Journal. 1980; 26(3): 379-386. doi: 10.1002/aic.690260308
15. Figueiredo JL, Moulijn JA. Carbon and Coal Gasification. Springer Netherlands; 1986. doi: 10.1007/978-94-009-4382-7
16. van Heek KH, Mühlen HJ. Fundamental Issues in Control of Carbon Gasification Reactivity. In: Lahaye L, Ehrburger P (editors). Fundamental Issues in Control of Carbon Gasification Reactivity. Kluwer Academic Publishers; 1991. pp. 1-34.
17. Kaufman Rechulski MD, Schneebeli J, Geiger S, et al. Liquid-Quench Sampling System for the Analysis of Gas Streams from Biomass Gasification Processes. Part 1: Sampling Noncondensable Compounds. Energy & Fuels. 2012; 26(12): 7308-7315. doi: 10.1021/ef3008147
18. Kaufman Rechulski MD, Schneebeli J, Geiger S, et al. Liquid-Quench Sampling System for the Analysis of Gas Streams from Biomass Gasification Processes. Part 2: Sampling Condensable Compounds. Energy & Fuels. 2012; 26(10): 6358-6365. doi: 10.1021/ef300274p